

Dual band- dual beam reduced size Butler matrices

N. M. JIZAT^a, S. K. A .RAHIM^b, M. I. SABRAN^b

^aFaculty of Engineering, Multimedia University, 63100 Cyberjaya, Selangor, Malaysia

^bWireless Communication Centre, Faculty of Electrical Engineering, Universiti Teknologi Malaysia, 81310 UTM Skudai, Johor, Malaysia

Beam forming vector are calculated to track and locate the antenna beam on the target are becoming popular demand to cope with the growing demand for supportable peak data rates, coverage requirements, and capacity objectives, as well as exciting new and enhanced applications. The system provides a broad range of ways to improve the performance of wireless communication systems, thus characterized as some of the most promising devices in wireless communications. While this revolution is significantly expanding the opportunity for new, smaller and better wireless communication terminals, it also is creating new performance demands for antennas. The implementation of beamforming network as one of smart antenna medium in future wireless systems is anticipated to have a significant impact on the efficient use of the spectrum, the minimization of the cost of establishing new wireless networks, the optimization of service quality, and recognized of transparent operation across multi technology wireless networks. Furthermore, smart antennas improve call quality on both forward and reverse links. Thus, reduced- size cascaded Butler matrices are developed for dual-band and dual-beam applications are presented in this paper using meander-line technique, an acceptable approach for reducing the size of the radio frequency element. Compared with the conventional size, the proposed branch-line coupler (BLC) were reduced in size by 63 % and 56 % at 2.45 GHz and 5.8 GHz, respectively. The proposed, cascaded Butler matrices have the ability to exhibit two types of beams, i.e., narrow and broad, by feeding the signal into the respective input port of the Butler matrix. A meander line branch-line coupler with an area of 96 mm × 125 mm was used to replace the conventional, straight transmission line. This reduced the area of the Butler matrix by 36% compared to the conventional matrix. The actual measurements showed very good agreement with the results obtained from simulations.

(Received May 28, 2013; accepted January 22, 2014)

Keywords: Branch-line coupler, Butler matrix, Cascaded Butler matrices, Dual band, Wireless communication, Meander line

1. Introduction

The implementation of smart antenna techniques in future wireless systems is anticipated to have a significant impact on the efficient use of the spectrum, the minimization of the cost of establishing new wireless networks, the optimization of service quality, and recognized of transparent operation across multi technology wireless networks. Beam forming vector are calculated to track and locate the antenna beam on the target. Furthermore, smart antennas improve call quality on both forward and reverse links. Combinations of short-range and long-range systems for vehicle applications are realized by the innovation of continuous air-interface for long- and medium-range telecommunication (CALM)[1] where the system uses a protocol that allows the system in the vehicle to switch to the appropriate telecommunication system that is accessible at that specific time. For this reason, the CALM concept is applicable for intelligent transportation system (ITS) applications with access to more than one communication system. Such a system, when incorporated into a network, provides a powerful platform that can be used to avoid and sense collisions. The system requires an immediate reaction for two-way communication links, especially for time-critical safety communications and supplementary ITS-specific network platforms, where required.

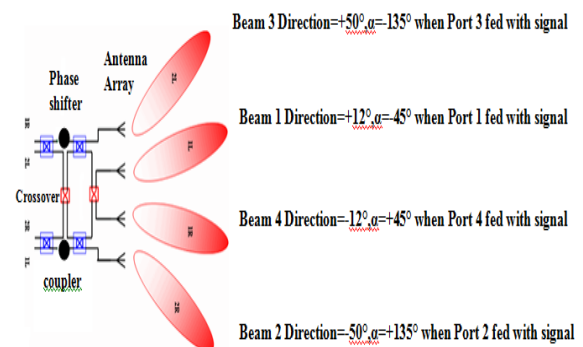


Fig.1. Phasor excitation and beam direction of a Butler matrix.

Phases are added constructively to create the radiation pattern of the antenna array where the signals are directed to the desired target and nulling the pattern of the undesired. Figure 1 shows the topology of the Butler matrix, consist of BLC, a crossover, and a phase shifter. The beam direction is illustrated with respect to each input ports.

2. Butler Matrix Structure

A new design is proposed that optimizes the size of the Butler Matrix. Butler Matrix is a beam forming network that employed a combination of 90° hybrids and phase

shifter, where a spatial Fast Fourier Transform (FFT) which can provide $2n$ orthogonal beams is satisfied [2-9]. The array elements pattern produced beams with linearly independent combinations. Butler Matrix is a network that control amplitudes and phases of the excitation for the smart antenna. The signal fed to each input port of the Butler Matrix is segregated to four output ports with equal amplitude and specified relative phase differences, accordingly generating four different beams through the smart antenna array connected.

2.1 Dual-Band BLC with reduced size

BLC takes up over 50% of the planar area in Butler matrix as the coupler is the essential part in the design. The dimension of coupler employs a quarter wavelengths square and occupies a significant amount of the board area. In order to reduce the area of the proposed BLC, an array of coupled, parallel, transmission lines, known as meander lines are applied. This approach uses meander lines and operates at two widely separated frequency bands ($f_2 > 2f_1$). BLC is designed with partially meandered line, implying that the meander line is only implemented at its shunt arm; while the through line uses normal line impedance. Moreover, lower inductance and capacitance are achieved since the length of a reduced-line is less than one-quarter

wavelength. The inductance drop can be compensated by increasing the characteristic impedance of the line through meander line. The meander line is used as the shunt arm of the proposed BLC.

Compared with the conventional dual-band BLCs in [10] and [11], the areas were reduced by approximately 65% and 90%, respectively, with comparable performances. A size reduction of 90% was a significant achievement for a design that has such a widely-separated frequency band.

In addition, the meander lines are represented as equivalent circuits of inductors, the equivalent circuit forms the basis for assembling the meander lines [12]. In the proposed coupler structure shown in Fig. 2, meandered lines were introduced to substitute for the shunt arm for generating a multi-band response, subsequently decreasing the size of the dual-band component dramatically.

In the proposed coupler structure, six M are used with M are resembled as one node in meander line analogy as clearly seen in the Table 1. Meander-line geometry are applied at the shunt arms to prevent overlapping and overcrowded at the centre area of the coupler. Theoretically, deterioration of coupler performance can be avoided, which was encountered by previous researchers. The proposed coupler was simulated by CST Microwave Studio[®] with the dimensions shown in Table 2.

Table 1. Two port equivalent circuits for meander lines.

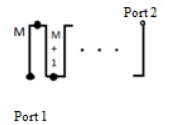
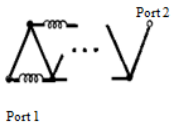
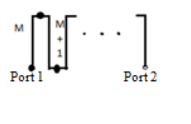
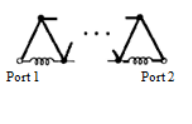
	ORIGINAL CIRCUIT	EQUIVALENT CIRCUIT
M ODD		
M EVEN		

Table 2. Dimensions of the Meander Branch Line Coupler.

Parameter	L1	L2	L3	S1	S2	S3	W1	W2
Value (mm)	5.45	1.90	9.65	0.30	2.20	4.20	0.50	2.35

2.2 Crossover design

The design of the crossover generally is conducted in such a way that the lowest value of coupling is exhibited [13]. Rather than using the conventional approach in this study, the crossover is achieved by cascading two couplers. In fact, the crossover determines the minimum value of isolation required for achieving good coupling performance. Afterwards, optimization is performed by adjusting the length of the interconnection, which provides the best isolation for realizing ideal reflections and coupling.

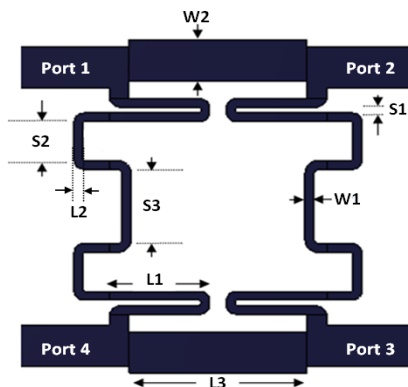


Fig. 2. Geometry and dimensions of the proposed coupler.

2.3 Phase Shifter

Broadband phase and amplitude balance can be achieved by using various configurations of Schiffman's phase shifter. Thus, Schiffman phase shifters are implemented in the design of dual band Butler Matrix as a solution of broad banding phase shift which can covered the desired phase at required frequencies, 2.45GHz and 5.8GHz respectively.

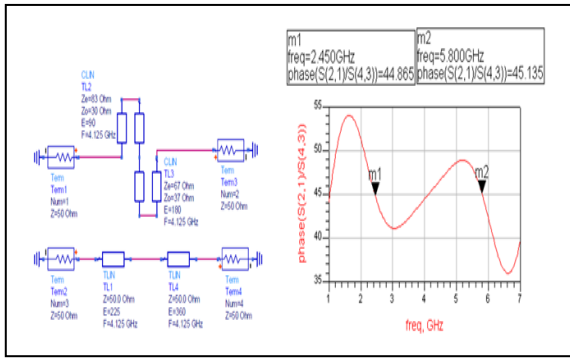


Fig. 3. Schematic and simulated phase difference result of 45° Schiffman phase shifter.

45° Schiffman broad-band phase shifter schematic structure is presented as shown in Fig. 3. The phase shifter is one four port network with two separate branches. One branch is a section of reference transmission line, and the other comprises a symmetrical coupled-lines section with one end, called the C-section network, connected.

Phase shifters are key components that are extensively used in scanning phased arrays. As shown in Fig. 4, the meander line can be considered as a repetitive structure of a unit cell. Table 3 shows the dimensions of an optimized meander line for the phase shifter. Each parameter is tuned in adequate-distance order to attain the desired phase shift, which operates at dual-band frequencies. In designing a 45° phase shifter, the width, W1, of the meander line is 2.34 mm, and the spacing gaps, S1 and S2, are 4 mm and 3 mm, respectively, as indicated in Fig. 6 (a). The meander length has a feature of L1 = 13.5 mm.

Meanwhile, the parameters of a 135° phase shifter are presented in Fig. 5 (b) with respect to four different values of each parameter. In this work, the spacing gaps, S1 and S2, of the meander line were fixed at 3.40 mm and 1.91 mm, respectively. It was found that the meander line that had a width and a length of 2.34 mm and 16.50 mm, respectively, gave the best phase shift at the desired frequencies.

Table 3. Dimensions of the Meander Phase Shifter in mm.

	S1	S2	L1	W1
45°	4.00	3.00	13.50	2.35
135°	3.40	1.91	16.5	2.35

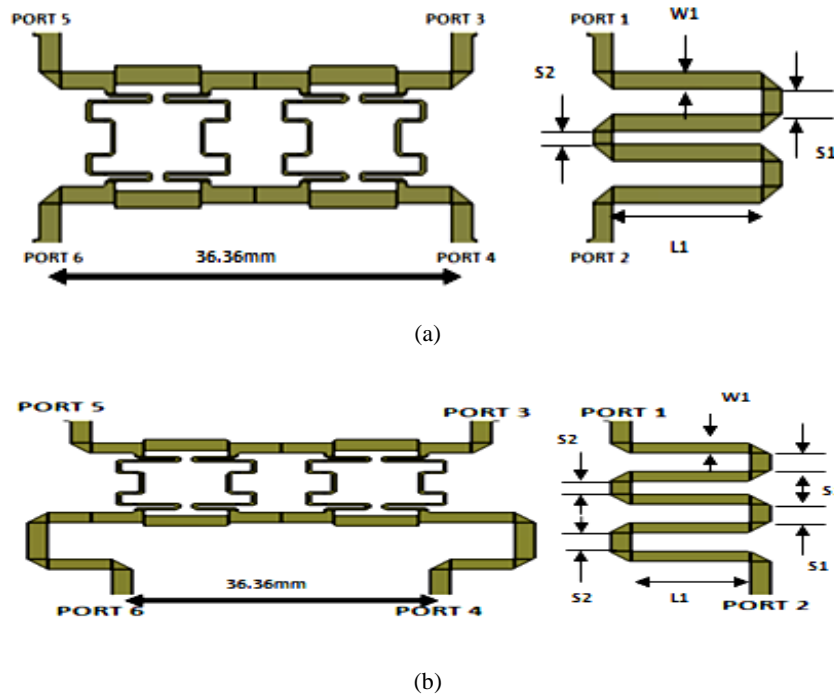


Fig. 4. Layout design of (a) 45° Schiffman Phase Shifter and (b) 135° Phase Shifter.

The output result between ports [S (2,1)/S(6,3)] should yield the value of 135° between the ports. In this design, it was considered that the constant phase spacing between the output ports was $\lambda_o/2 = 36.36$ mm. The spacing, λ_o , specified in Equation (1) matches the antenna array with the same element spacing in which c represents the velocity of light, 3×10^8 m/s, at a centre frequency, f_o , of 4.125 GHz

$$\lambda_o = \frac{c}{f_o} \quad (1)$$

2.4 Butler Matrix

The proposed 4×4 Butler matrix was implemented as a passive microstrip network on the substrate FR4. The phase shifts required by the network were generated using microstrips. When one of the input ports was excited by an RF signal, all the output ports feeding the array elements

were equally excited, though with a progressive phase between them, resulting in radiation of the beam at a certain angle. As different input ports were excited, the Butler matrix was treated as a beam forming network, which provided four output signals with equal power levels and with progressive phases of $+45^\circ$, -45° , $+135^\circ$, and -135° . Hence, the user can switch the direction of the main radiation beam by exciting the designated input port. The system is capable of producing multiple narrow beams in different directions and thereby selecting the strongest signal among all of the available signals. The scheme of the proposed, dual-band Butler matrix design is shown in Fig. 5 (a). A photograph of the implemented concept of the Butler matrix circuit is shown in Fig. 5(b). The size of the prototype branch line coupler was $111 \text{ mm} \times 170 \text{ mm}$.

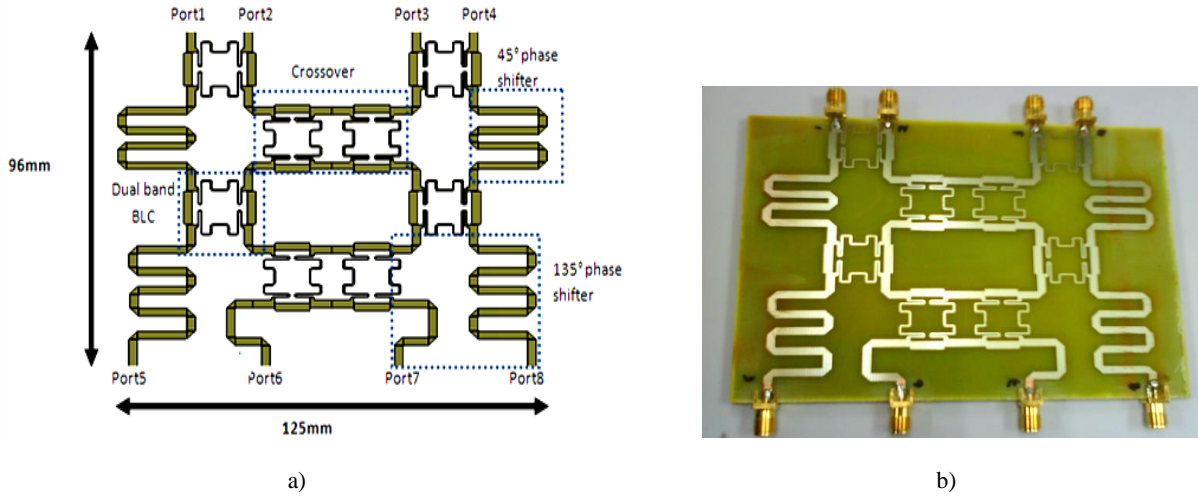


Fig.5. Proposed Butler matrix (a) layout and (b) prototype.

3. Results and discussion

Performances of proposed dual-band branch-line coupler (BLC) in the form of simulated and measured results are presented. The branch-line coupler is fabricated on FR4 (dielectric constant, $\epsilon_r = 4.6$, dielectric height, $H = 1.6$ mm, metal thickness, $T = 0.035$ mm, loss tangent = 0.019 and copper conductor). Simulated and measured results of the branch-line coupler show reasonable good agreement.

Fig. 6 presents the simulated and measured performances of the proposed couplers. The slight discrepancies observed may be due to fabrication issues, especially at high frequency. Referring to return loss, S_{11} , and isolation, S_{41} , the branch line coupler had good values (less than -10 dB) across the dual-band frequencies, which is an indication of a good transmission output signal. Compared to the simulated results, the measured values were approximately 5 dB and 10 dB better at the lower and higher frequencies, respectively. The performance at both operating frequencies is summarized in Table 4.

Equations (2) and (3) give the expression for -10dB bandwidth calculation. For lower band, the calculated

bandwidth is 18.42%, and it covers frequency range from 1.94 GHz to 2.70 GHz. On the other hand, for upper band, the calculated bandwidth is 15.51% and it covers a range from 5.55 GHz to 6.19 GHz.

$$BW = \frac{f_2 - f_1}{f_c} \times 100\% \quad (2)$$

$$f_c = \frac{f_1 + f_2}{2} \quad (3)$$

From the results of the measurements, return loss, S_{11} , was -24.5 dB at 2.45 GHz (lower frequency); whereas the value was -14.9 dB at 5.8 GHz (upper frequency). The measurement showed that the magnitudes of insertion losses, S_{21} , and coupling, S_{31} , were -4 dB and -3 dB, respectively, at each frequency. The measured value of -3 dB indicated that power was divided equally between the output ports of the coupler. The isolation values, S_{41} , were -16.8 dB and -25.1 dB, respectively, at 2.45 GHz and 5.8 GHz. The most important challenges in coupler design are equal power division and accurate phase difference determination. The phase differences are approximately

89° and 88° at 2.45 GHz and 5.8 GHz, respectively. The measured values of insertion losses, S_{21} , and coupling, S_{31} , at 2.45 GHz and 5.8 GHz respectively, indicate that the branch-line coupler successfully provided an equal 3-dB split, within measurement accuracy, and had a 0.9-dB loss

at the resonant frequencies. Due to good response of the measured characteristics, this design was selected as a fundamental component for implementing the dual-band, dual-beam, reduced-size Butler matrix.

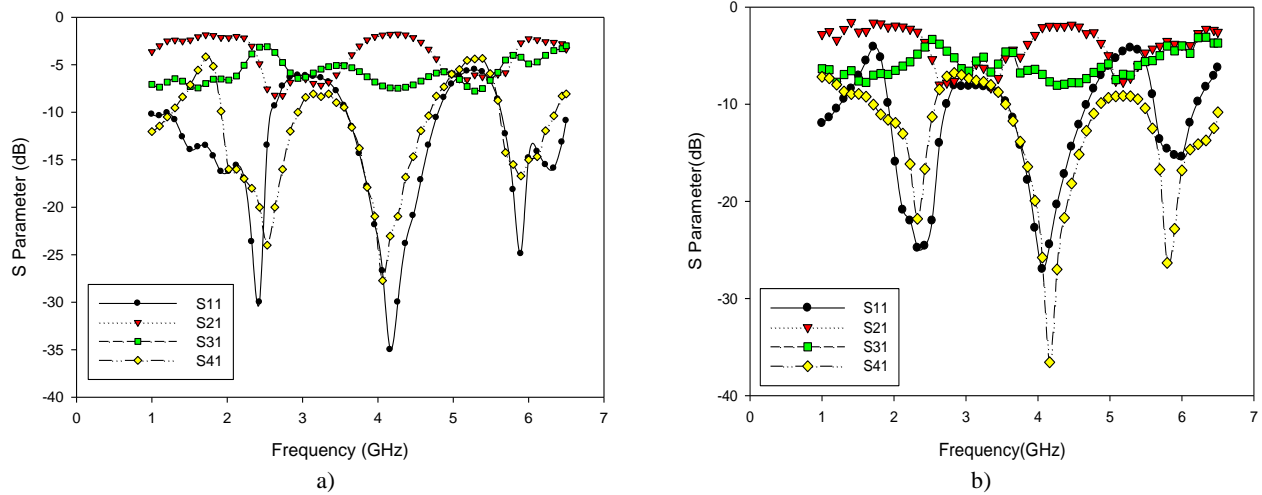


Fig. 6. S-parameters of the proposed dual band BLC (a) simulation and (b) measurement.

Table 4. Performance of the proposed coupler.

S-parameter		Return Loss (S_{11}) dB	Output 1 (S_{21}) dB	Output 2 (S_{31}) dB	Isolation (S_{41}) dB	Phase Difference (°)	-10dB Bandwidth (%)
Simulation	2.45GHz	-30.0	-3.99	-3.59	-21.8	90.3	24.24
	5.8 GHz	-24.3	-3.39	-3.89	-15.0	87.7	18.33
Measurement	2.45GHz	-24.5	-3.90	-3.89	-16.8	89.0	18.42
	5.8 GHz	-14.9	-3.99	-3.89	-25.1	88.0	15.51

From the results of the measurements, return loss, S_{11} , was -24.5 dB at 2.45 GHz (lower frequency); whereas the value was -14.9 dB at 5.8 GHz (upper frequency). The measurement showed that the magnitudes of insertion losses, S_{21} , and coupling, S_{31} , were -4 dB and -3 dB, respectively, at each frequency. The measured value of -3 dB indicated that power was divided equally between the output ports of the coupler. The isolation values, S_{41} , were -16.8 dB and -25.1 dB, respectively, at 2.45 GHz and 5.8 GHz.

Power division is important for accurate phase difference determination in BLC. The phase differences are approximately 89° and 88° at 2.45 GHz and 5.8 GHz, respectively, as clearly shown in Fig. 7. The measured values of insertion losses, S_{21} , and coupling, S_{31} , at 2.45 GHz and 5.8 GHz respectively, indicate that the branch-line coupler successfully provided an equal 3-dB split, within measurement accuracy, and had a 0.9-dB loss at the resonant frequencies. Due to good response of the measured characteristics, this design was selected as a fundamental component for implementing the dual-band, dual-beam, reduced-size Butler matrix.

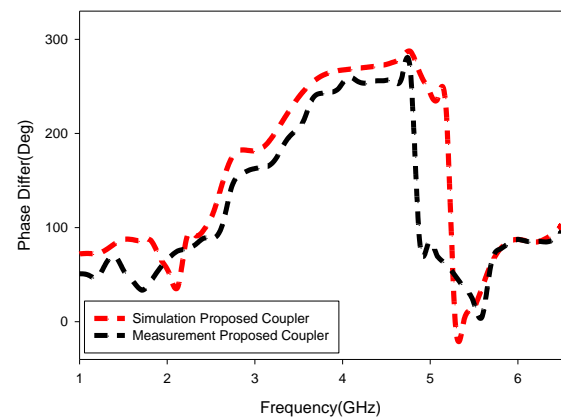


Fig. 7. Phase difference response between output ports of the proposed meandered coupler.

An antenna array is developed for a certain spacing to produce directional radiation pattern. The radiating pattern depends on the configuration, the distance between the elements, the amplitude and phase excitation of the elements, and additional factor it depends on radiation pattern of individual elements. Array factor are identified from the radiation pattern of the array excluding

the individual element pattern and can be achieved by considering the elements to be point sources as illustrated in Fig. 8. The array factor can be given as (4-6):

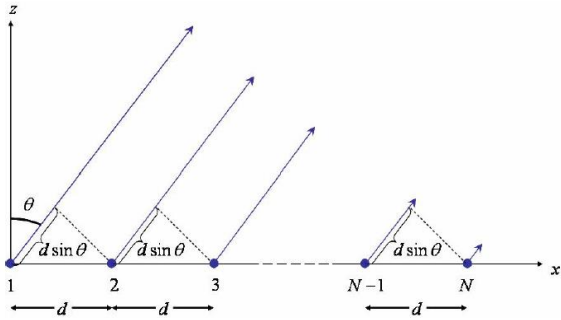


Fig. 8. N -element array of elements along z -axis.

$$AF = 1 + e^{+j(kd \cos \theta + \beta)} + e^{+j2(kd \cos \theta + \beta)} + \dots + e^{+j(N-1)(kd \cos \theta + \beta)} \quad (4)$$

$$AF = \sum_{n=1}^N e^{+j(n-1)(kd \cos \theta + \beta)} \quad (5)$$

$$AF = \sum_{n=1}^N e^{+j(n-1)\varphi} \quad (6)$$

where $\varphi = kd \cos \theta + \beta$

In order to monitor the array factor and the field of the array, separation, d or the progressive phase shifts are varied continuously between the elements. Array structure has four elements spaced by $0.5 \lambda_0$ are employed at 2.45 GHz and 5.8GHz in reducing the mutual coupling between elements by achieving minimum level side lobes. As a result, the array has uniform amplitude distribution and constant phase shift between adjacent elements to generate orthogonal beams.

A few experimental result showed that element spacing; greater than a half wavelength, causes some sidelobes to become substantially larger in amplitude, and approaching the level of the main lobe. In such a case, the best spacing of half wavelength made the sidelobes reduced in order to maintain the main beam performance. The signal constructed is amplified by constructive interference in the main direction while the beam sharpness is improved by the destructive interference.

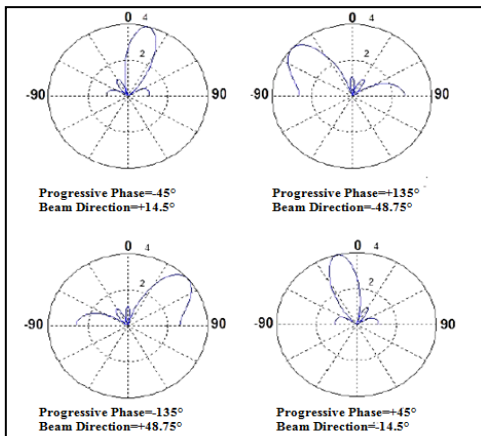
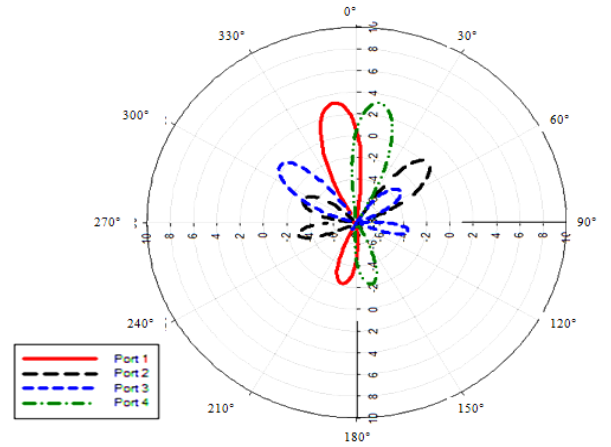
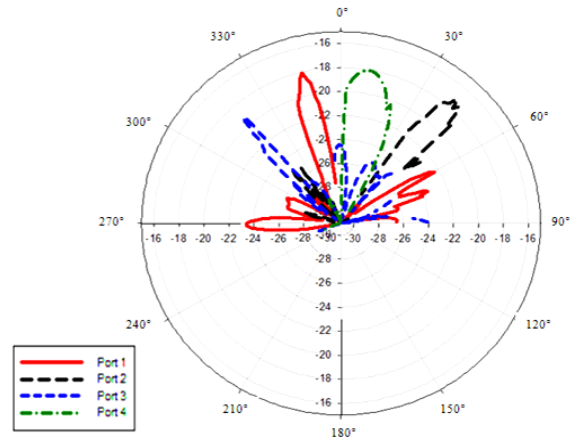


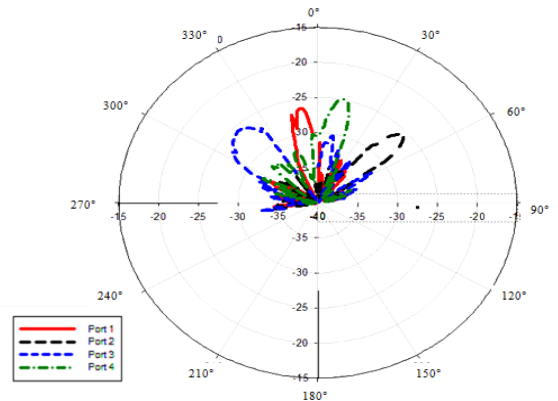
Fig.9. Simulated radiation patterns with various progressive phase shifts



(a)



(b)



(c)

Fig.10. Radiation Patterns (a) Simulated beam direction for each of the ports at 2.45 and 5.8 GHz, (b) Measured beam direction for each of the ports at 2.45 GHz, (c) Measured beam direction for each of the ports at 5.8GHz.

Fig. 9 illustrates the simulated radiation patterns beam directions for various progressive phase shifts using MATLAB simulator in which the array structure has four elements spaced by $0.5 \lambda_0$ at 2.45 GHz in order to minimize the mutual coupling between elements and to obtain the minimum level side lobes. As a result, the array has uniform

amplitude distribution and constant phase shift between adjacent elements to generate orthogonal beams. The radiation pattern of the array excluding the element pattern is referred to as the array factor. The mid-frequency applied in this project is 4.125GHz, so that the wavelength λ contribute to 0.07272 m. Since this project emphasize the application of 4x4 Butler Matrix, the number of elements and the distance between elements are 4 and $\lambda/2$ respectively.

Fig. 10(a) shows the simulated beam direction for each of the ports at 2.45 GHz and 5.8 GHz. The measured and simulated results showed that real antenna dimensions and non-zero spacing angle influence the bearing precision in the angle range of 0° to 180° . It is possible to use the proposed matrix for determining the sector bearing set. Therefore, four patch antenna arrays were dedicated to work with the proposed Butler matrix.

The selection of the input port of the Butler matrix will activate the respective beams at the radiating part. By turning on the first input at 2.45 GHz, the beam direction was altered by -14° with HPBW from -10° to -19.6° , as shown in Figure 10(b). On the other hand, if the signal were fed to input port 2, the maximum radiation direction was achieved at 42.33° , with HPBW from 37.04° to 47.37° . When Port 3 input signal was inserted, the output beam was pointed directly at -42° with a signal with an HPBW ranging from -40° to -45° , while the beams are altering to 11.06° when port 4 is fed, with the resulting HPBW of 2 to 22.41° . The beam direction at 5.8 GHz is demonstrated in Figure 10(c). It was observed that narrow beam widths were generated from the estimated value of HPBW, with the HPBW varying from minimum range (5°) to the maximum range (21.4°).

The measurement and simulation results are fairly comparable. Nevertheless, the direction of the measured beam differed slightly from the actual direction. This discrepancy may have occurred due to the phase differences at the output ports being disturbed by the fringing effect cause by fringing fields around the radiating elements. As a result, the measured beams were slightly lower than the simulated beams. Even though slight differences were observed in these scenarios, the results proved that the proposed, dual-band Butler matrix can produce four beams across dual-band, WLAN frequencies at respective beams.

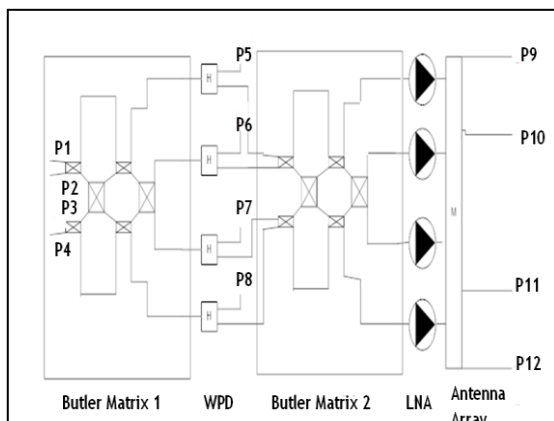


Fig. 11. Topology of design system.

Briefly discussed, as illustrated in Fig. 11, 4x4 Butler Matrix microwave beamforming network has been cascaded back to back in order to produce narrow-beams and broad-beams suitable for beam scanning electronically steered arrays. Signals entering the input ports of the first Butler Matrix 1 beamforming network (P1-P4) are subdivided into equal amplitude with progressive phase variation across the output ports, for high-gain narrow-beam reception that are potential for long-range communication.

The respective signals are then fed into the Wilkinson Power Dividers (WPD). The signal from one end of each WPD forms a narrow output beam(P5-P8) while the signals from the other ends of the WPD are fed into the second Butler Matrix to regenerate the broad-beam characteristics of the individual radiating elements. The active antenna consists of a Low-Noise Amplifier (LNA) coupled to a low-profile planar meanderline Butler Matrix. As a result, high-gain and broad-beams are produced on the output ports of the second Butler Matrix beamforming network that are suitable for short-range communication.

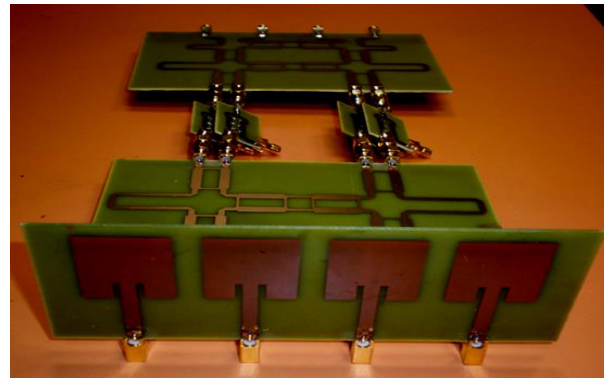


Fig. 12. Integration of reduced-size, dual-band, dual-beam Butler matrix prototypes.

Fig. 12 illustrates the proposed Butler Matrices that produces dual-beam, dual-band application that can be used for both long range and short range applications. This target application is specifically for roadside-vehicle communications and inter-vehicle communications.

The narrow beams presented in the first Butler matrix can be used to switch the main beam in the desired signal directions, while directing null in the interference directions. Radiation pattern measurements were performed to obtain the desired beams that can operate simultaneously at 2.45 GHz and 5.8 GHz. Figure 10 illustrates four beams with respect to each of the input ports for both the simulated and measured Butler matrix.

Figs. 13 (a) and (b) illustrate the simulated and measured array factors at 2.45 GHz, respectively while Figures 14 (a) and (b) illustrate the simulated and measured beam patterns from the cascaded Butler matrix at 5.8 GHz, respectively. Broad-beam patterns were generated from the output ports of the second Butler matrix when the input ports of the first Butler matrix were fed with signals. This is the reaction of the second Butler matrix acting as a mirror of the first Butler matrix, reconstructing the antenna patterns of the individual radiating element. The measured radiation patterns agreed with the values of the simulated array factors in terms of the direction of the main beam.

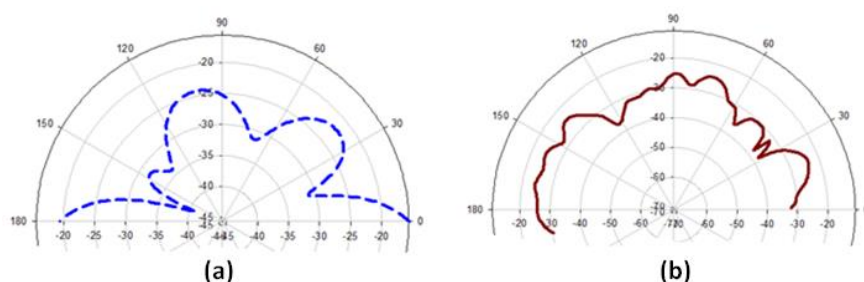


Fig. 13. Radiation pattern broad beamwidth at 2.45 GHz, (a) Simulation, (b) Measurement.

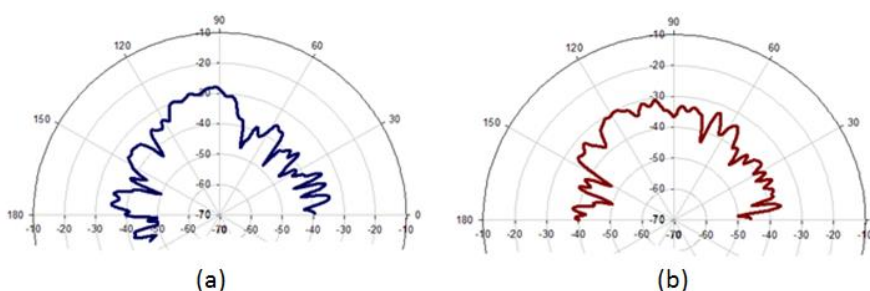


Fig. 13. Radiation pattern broad beamwidth at 5.8 GHz, (a) Simulation, (b) Measurement.

4. Conclusion

The major contributions of the study include extensive reductions in the size and manufacturing cost. The methodology enables branch-line coupler to reduce in area by 34% from the previous design using planar dual band BLC without having to compromise circuit performances. Another merit is the proposed system entitled with low cost, small volume, and light weight. These features make the proposed Butler matrix suitable for WLAN applications at 2.45 GHz and 5.8GHz. In addition, this design realized on the FR4 board offers an excellent return loss and coupling output responses at desired frequency. Developing sector beaming system makes easier elimination of internal interferences between antenna systems and reduced frequency characteristics elements of matrix by minimising amplitude-phase transformation level receiving signals. With these results outcome of this project summarise that presented system can be very efficient for detecting of short-time emission.

References

- [1] N. Wall, ITS Comms. The CALM and Efficient Way. Traffic Engineering & Control Magazine, 2006.
- [2] J. L. Butler, R. Lowe, Electronic Design. **12**, 170 (1961).
- [3] N. M. Jizat, S. K. A. Rahim, T. A. Rahman. Dual and Beamforming Network Integrated with Array. Fourth Asia International Conference on Mathematical/Analytical Modelling and Computer Simulation. 561 (2010).
- [4] A. Angelucci, P. Audagnotto, P. Corda, B. Piovano. Antennas and Propagation Society International Symposium, 628 (1994).
- [5] M. Dessouky, H. Sharshar, Y. Albagory, Journal of Electromagnetic Waves and Applications, PIER. **21**(13), 1721 (2007).
- [6] W. Liu, R. Langley, Adaptive wideband beamforming with combined spatial/temporal sub-band decomposition. PIERS Online, 2007.
- [7] G. S. Liao, H. Q. Liu, J. Li, A subspace-based robust adaptive capon beam forming. PIERS Online. Cambridge, USA, **2**(4), 374 (2006).
- [8] L. Accatino, A. Angelucci, B. Piovani, Microwave Engineering Europe. 45–50 (1992).
- [9] T. Denidni, T. Libar, Personal, Indoor and Mobile Radio Communications, 3 (2003).
- [10] M. Hayati, M. Nosrati, Progress In Electromagnetics Research C., PIER. **10**, 75 (2009).
- [11] M. J. Park, B. Lee, IEEE Microwave Wireless Compon Lett. IEEE, **15**(10), 655 (2005).
- [12] N. M. Jizat, S. K. A. Rahim, T. A. Rahman, A. Y. Abdulrahman, M. I. Sabran, P. S. Hall, Microwave and Optical Technology Letters, **53**(11), 2543 (2011).
- [13] J. S. Wight, W. J. Chudobiak, IEEE Trans. On Microwave Theory and Techniques, 270 (1976).